

Validation, Verification and Calibration in Applied Computational Electromagnetics

Gökhan Apaydin¹ and Levent Sevgi²

¹Department of Electrical and Electronics Engineering
Zirve University, Gaziantep, 27260, Turkey
gokhan.apaydin@zirve.edu.tr

²Department of Electronics and Communications Engineering
Dogus University, Acibadem, Istanbul, Turkey
lsevgi@dogus.edu.tr

Abstract — Model validation, data verification, and code calibration (VV&C) in applied computational electromagnetics is discussed. The step by step VV&C procedure is given systematically through canonical scenarios and examples. Propagation over flat-Earth with linearly decreasing vertical refractivity profile, having an analytical exact solution, is taken into account as the real-life problem. The parabolic wave equation (PWE) is considered as the mathematical model. MatLab-based numerical simulators for both the split step Fourier and finite element implementations of the PWE are developed. The simulators are calibrated against analytical exact and high frequency asymptotic solutions. Problems related to the generation of reference data during accurate numerical computations are presented.

Index Terms — Calibration, finite elements method, geometric optics, groundwaves, mode method, narrow angle, parabolic equation method, propagation, split step parabolic equation method, validation, verification, wide angle.

I. INTRODUCTION

Real life engineering and electromagnetic (EM) problems can be handled via measurements or numerical simulations because only a limited number of problems with idealized geometries have mathematical exact solutions. The challenge in solving real-life engineering problems is

therefore the reliability of the results. Reliability is achieved after a series of (model) validation, (data) verification, and (code) calibration (VV&C) tests. These issues are discussed in [1] and this paper is the extended version of that presentation.

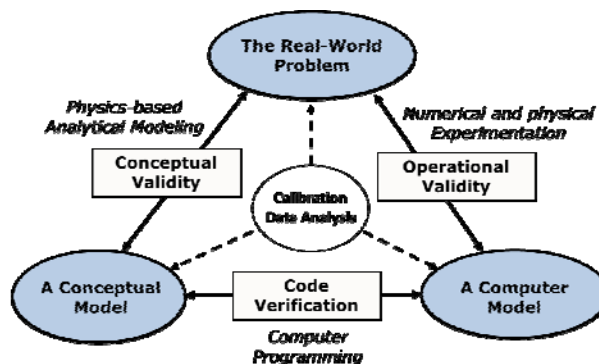


Fig. 1. Fundamental VV&C concepts & procedures.

Three fundamental building blocks of a simulation are the real-world problem entity being simulated, the conceptual model representation of that entity, and the computer implementation model. As illustrated in Fig. 1, engineers start with the definition of the real-life problem at hand. Electromagnetic problems, in general, are modeled with Maxwell's equations and EM theory is well-established by these equations. Maxwell's equations are general and represent all linear EM problems. Once the geometry of the problem at hand (i.e., boundary conditions, BC) is given, they represent a unique solution; the solution found by

using Maxwell's equations plus BC is the solution we are looking for. Unfortunately, there are only a few real-life problems which have mathematically exact solutions therefore many different and approximate conceptual models can be used. It is the process of conceptual validity which shows that chosen conceptual model fits into the real-life problem best under the specified initial and/or operational conditions. The next step is to develop a computer code for the chosen conceptual model. It is only after this that code verification via a computer programming process may be applied to show that the developed code represents the chosen conceptual model under given sets of conditions (accuracy, resolution, uncertainty, etc.). Finally, the solution for the real-life problem is obtained with a confidence after numerical and/or physical experimentation; nothing but the operational validity process [2].

The suitability (validation) of the conceptual model and verification of the software and synthetically generated data are the technical processes that must be addressed to show that a model is *credible*. Credibility is based on two important checks that must be performed in every simulation: validation and verification. Validation is the process of determining that *the right model is built*, whereas verification is designed to see if *the model is built right*. The final step of the verification is the calibration.

The VV&C procedure in applied computational electromagnetics is discussed here. The real-life problem chosen for this purpose is the two-dimensional (2D) propagation over flat-Earth with a perfectly electrical conductor (PEC) surface through a non-homogeneous atmosphere. The linearly decreasing vertical refractivity profile under these circumstances yields an analytical exact solution. There are many conceptual/mathematical models which might fit into these conditions; one of them, the parabolic wave equation (PWE), is chosen as the test model. MatLab-based numerical simulators for both the split step Fourier and finite element implementations of the PWE are developed. The VV&C procedure necessitates quantitatively and qualitatively answering these questions: (i) How precise is the PWE model? (ii) To what extent does the PWE correspond to the real-life problem? (iii) Under what/which conditions do SSPE and FEMPE yield reliable solutions? (iv) What is the

accuracy of the numerical calculations? In order to answer these questions and similar ones, one needs to generate a reference data and systematic comparisons. Here, the simulators are calibrated against analytical exact (in terms of modal summation) and high frequency asymptotic (in terms of geometric optic (GO)-ray summation) solutions. Problems related to the generation of reference data during accurate numerical computations are presented. Then, the problems related to model simplifications and inadequacy, model truncation (because of a finite number of modes taken into account), and error introduced from improper discretization are all discussed.

II. PARABOLIC EQUATION MODEL FOR GROUNDWAVE PROPAGATION PROBLEM

The PWE has become a classical tool in modeling groundwave propagation problems. It is derived from the 2D Helmholtz's equation by separating rapidly varying phase term in a medium to obtain an amplitude factor which varies slowly in range when the direction of propagation is predominantly along $+z$ paraxial direction under $\exp(-i\omega t)$ time dependence [3-7]

$$\left\{ \frac{\partial^2}{\partial z^2} + \frac{\partial^2}{\partial x^2} + 2ik_0 \frac{\partial}{\partial z} + k_0^2(n^2 - 1) \right\} u(z, x) = 0, \quad (1)$$

where $u(z, x)$ denotes the wave amplitude either of the electric or magnetic field components for horizontal and vertical polarization respectively; $k_0 = 2\pi/\lambda$ is the free space wavenumber, n is the refractive index, x and z stand for the transverse and the longitudinal coordinates, respectively (note that, PWE was first introduced in acoustics [3] and since then has been applied to a huge number of propagation problems not only in acoustics but also in electromagnetics and optics and has become classical. None of the lists of references would be complete on the PWE topic; therefore, the reader is referred to in [4] and the references there to initiate a literature search. If the refractive index is range-independent and backward propagation is ignored, (1) reduces to

$$\left\{ \frac{\partial}{\partial z} + ik_0(1 - \sqrt{1+q}) \right\} u(z, x) = 0, \quad (2)$$

where $q = k_0^{-2} \partial^2 / \partial x^2 + (n^2 - 1)$. If the angle of propagation measured from the paraxial direction

is less than 15° , the standard parabolic equation (PE) can be used with the help of square root approximation ($\sqrt{1+q} \approx 1+q/2$). If this angle is more than 15° , Claerbout equation can be obtained by using the first order Padé approximation ($\sqrt{1+q} \approx (1+0.75q)/(1+0.25q)$) to satisfy the propagation angle up to 35° - 40° [4]. Hence, the PE is described as

$$\left\{ A_0 \frac{\partial^3}{\partial x^2 \partial z} + A_1 \frac{\partial}{\partial z} + A_2 \frac{\partial^2}{\partial x^2} + A_3 \right\} u(z, x) = 0, \quad (3)$$

with coefficients $A_0 = 0$, $A_1 = 2ik_0$, $A_2 = 1$, and $A_3 = k_0^2(n^2 - 1)$ for narrow angle case or $A_0 = 1$, $A_1 = k_0^2(n^2 + 3)$, $A_2 = -2ik_0$, $A_3 = -2ik_0^3(n^2 - 1)$ for wide angle case with one-way forward propagation.

Choosing the appropriate longitudinal BC

$$\left\{ \frac{\partial}{\partial z} - ik_0 \right\} u(z, x) \Big|_{z \rightarrow \pm\infty} \rightarrow 0, \quad (4)$$

and transverse BC

$$\left\{ \alpha_1(z) \frac{\partial}{\partial x} + \alpha_2(z) \right\} u(z, x) \Big|_{x=0} = 0, \quad (5)$$

with the flat-Earth assumption completes the definition of the conceptual model. Here, $\alpha_1(z)$, $\alpha_2(z)$ become constants for homogeneous path and $\alpha_j(z) = 0$ ($j=1,2$) results in Dirichlet (horizontal polarization) and Neumann (vertical polarization) boundary conditions (DBC and NBC), respectively for PEC surface.

Since waves propagating upwards either go to infinity or bent down because of the refractivity variations, the open boundary upward in height can be modeled by using artificial lossy layer with the help of Hanning window in order to eliminate reflection effects [4-8]. The PWE and its application under different circumstances are pictured in Fig. 2. As illustrated in the figure, the beauty of the PWE is that all curvature effects including irregular terrain can be modeled via refractivity perturbations. On the other hand, PWE is an initial value problem, therefore boundary conditions must be satisfied artificially [4].

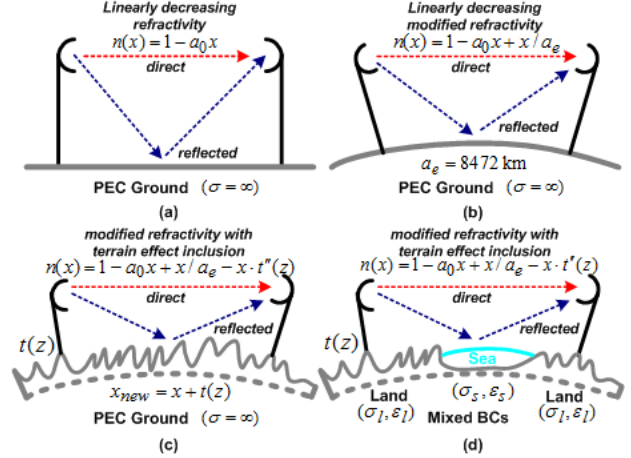


Fig. 2. 2D-PE modeling of groundwater propagation: a) flat Earth, b) Earth's curvature effect, c) irregular terrain effect, d) mixed boundary condition effect.

A. The split step parabolic equation (SSPE) propagator

The standard fast Fourier transform (FFT) based SSPE solution for narrow [4] and wide [5] angle, respectively,

$$u(z + \Delta z, x) = \exp \left[i \frac{k_0}{2} (n^2 - 1) \Delta z \right] \times \quad (6)$$

$$F^{-1} \left\{ \exp \left[-i \frac{k_x^2 \Delta z}{2k_0} \right] F \{ u(z, x) \} \right\},$$

$$u(z + \Delta z, x) = \exp [ik_0 (n - 1) \Delta z] \times$$

$$F^{-1} \left\{ \exp \left[\frac{-ik_x^2 \Delta z}{k_0 \left(1 + \sqrt{1 - k_x^2 / k_0^2} \right)} \right] F \{ u(z, x) \} \right\}, \quad (7)$$

can be used to calculate the vertical field $u(z + \Delta z, x)$ from $u(z, x)$ along z at range steps of Δz . The FFT based PE solution uses a longitudinally marching procedure. First, an antenna pattern representing the initial height profile is injected. Then, this initial field is propagated longitudinally from z_0 to $z_0 + \Delta z$ and the transverse field profile at the next range is obtained. This new height profile is then used as the initial profile for the next step and the procedure goes on until the propagator reaches the desired range. SSPE sequentially operates between vertical domain and the transverse domain. SSPE cannot automatically handle the BCs at Earth's surface. It is satisfied by removing the surface and taking a mirror copy of the initial vertical field

profile below (odd and even symmetric for DBC and NBC, respectively).

B. The finite element method based parabolic equation (FEMPE) propagator

The idea of FEM-based formulation of the PE is to divide the transverse domain into sub domains (called elements), use approximated field values at the selected discrete nodes in the vertical domain between ground and selected maximum height, and propagate longitudinally by the application of the Crank-Nicholson approach based on the improved Euler method which yields an unconditionally stable system and accurate method [8-10] starting from the initial field at $z=0$, which is generated from a Gaussian antenna pattern specified by its height (h_s), beamwidth (θ_{bw}), and elevation angle (θ_{ilt}).

Using (3), the matrix representation form of the FEMPE propagator is obtained as

$$\left[-A_0 K_{mj}^e + A_1 M_{mj}^e \right] \left\{ \partial c_j^e / \partial z \right\} + \left[-A_2 K_{mj}^e + A_3 M_{mj}^e \right] \left\{ c_j^e \right\} = \{0\}$$

for $M_{mj}^e = \int_{x_1^e}^{x_2^e} B_m^e B_j^e dx$, $K_{mj}^e = \int_{x_1^e}^{x_2^e} \frac{\partial B_m^e}{\partial x} \frac{\partial B_j^e}{\partial x} dx$, $e=1, \dots, n_e$, $m=1, \dots, d$, $j=1, \dots, d$ with the help of basis functions (B) of degree d where e stands for the elements, n_e is the number of elements in the vertical domain, and $c_j^e(z)$ denotes the coefficients of unknown functions. The DBC at the surface are satisfied by eliminating the first column and row of matrices since the initial node is always zero [9-10].

C. Typical applications of the SSPE and FEMPE propagators

The SSPE and FEMPE propagators are used to investigate various complex propagation problems [10-13]. Two examples are presented here in order to show the significance and requirement of the VV&C procedure in these problems. First, a typical irregular terrain path is generated and propagation above this irregular terrain through homogeneous atmosphere (including the Earth's curvature) is simulated under both DBC and NBC. Three dimensional (3D) field strength vs. range/height plot at 300MHz is pictured in Fig. 3. Only, the SSPE map is shown but the FEMPE map is also the same; it is almost impossible to distinguish the maps of both propagators. The source is a down-tilted Gaussian beam. As

observed, down propagation of the beam, reflection from the terrain, and interference between the direct and terrain-reflected waves are clearly observed. Moreover, the BC effects on the surface seem to be well-modeled [11-12].

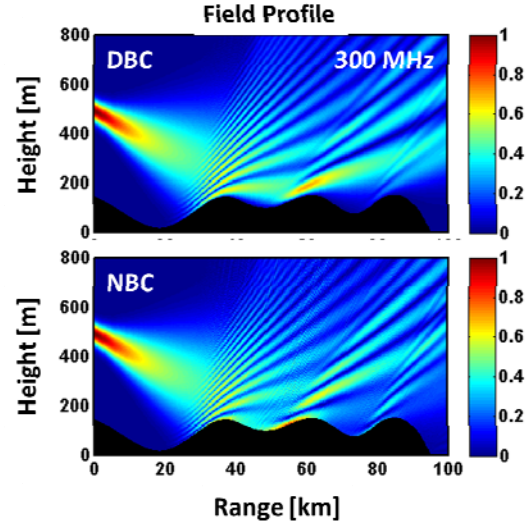


Fig. 3. Irregular terrain effect (PEC ground): 3D field map obtained via SSPE propagator under DBC and NBC ($h_s=350m$, $\theta_{bw}=0.5^\circ$, $\theta_{ilt}=-0.5^\circ$).

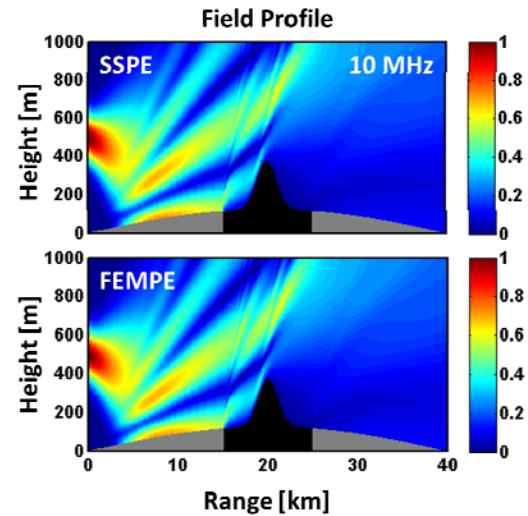


Fig. 4. Surface wave propagation: 3D signal vs. range/height map over a 3-segment 40km mixed path (a 10km long, 250m high Gauss-shaped island is 15km away from the transmitter) (Island: $\sigma = 0.002$ S/m, $\epsilon_r = 10$; Sea: $\sigma = 5$ S/m, $\epsilon_r = 80$).

The other example belongs to surface wave propagation over a three-section mixed-path (sea-land-sea) with a Gaussian shaped hilly island [12-13]. Surface wave propagation along this path at

10MHz generated via both propagators is shown in Fig. 4. Here, an elevated antenna is used (a Gaussian shaped antenna pattern with 5° vertical beamwidth, tilted 2° downwards, located 500m above the sea surface) is used to excite surface waves. As observed, waves hit the sea surface around 5km; energy couples to the surface and propagates thereafter. Also, observe how surface wave coupling in the near vicinity of the transmitter is important on the signal attenuation and range variations.

III. CANONICAL PROBLEMS AND GENERATING REFERENCE SOLUTIONS

The crucial questions in modeling and simulation as presented in the previous section are (i) Are they correct? (ii) How accurate are they? (iii) How can reliable comparisons be possible? The answer can only be given after a step by step, precise VV&C procedure. This section presents the generation of reference data which necessitates exact and/or asymptotic models as well as precise and accurate generation of reference numerical data.

A. Surface duct problem

Propagation over the PEC flat Earth with a linearly decreasing vertical refractivity profile (i.e. $n^2(x) = 1 - a_0 x$) is a canonical structure with analytical solutions in terms of Airy functions for the range-independent vertical refractive index. Here, a_0 is a positive constant which controls the strength of the duct. The exact modal solution of the Airy type wave equation using N modes is [2]

$$u(z, x) = \sum_{q=1}^N c_q Ai[(a_0 k_0^2)^{1/3} x - \sigma_q] e^{i\beta_q z}, \quad (8)$$

where c_q is the modal excitation coefficients, β_q is the longitudinal propagation constant for the related mode represented by index q as

$$\beta_q = \pm \sqrt{k_0^2 - (a_0 k_0^2)^{2/3} \sigma_q}, \quad (9)$$

Ai is the first kind of Airy function. The BC at the surface is satisfied with $Ai(-\sigma_q) = 0$ and $Ai'(-\sigma_q) = 0$ for the DBC and NBC, respectively. Here, the prime denotes the derivative with respect to the vertical coordinate. The problem is then reduced to find the modal excitation coefficients

from a given antenna pattern using orthonormality property from a given source function as:

$$c_q = \int_0^{x_{\max}} g(x) Ai[(a_0 k_0^2)^{1/3} x - \sigma_q] dx, \quad (10)$$

$$\text{where } g(x) = \frac{1}{\sqrt{2\pi\sigma^2}} \exp\left[-\frac{(x-h_s)^2}{2\sigma^2}\right].$$

Here, σ is the spatial width and h_s is the height of the Gaussian source $g(x)$. The Gaussian source pattern is often used in applications since it represents various antenna types (but any other source profile may also be used). The Gaussian antenna pattern can also be defined in the vertical wavenumber domain as

$$g(k_x) = \exp\left[\frac{-k_x^2 \ln 2}{2k_0^2 \sin^2(\theta_{bw}/2)}\right]. \quad (11)$$

The tilt (or elevation) angle (θ_{ilt}) is introduced by shifting the antenna pattern, i.e., $g(k_x) \rightarrow g(k_x - k_0 \sin \theta_{ilt})$. The vertical field in the spatial domain is then obtained by taking the inverse Fourier transform of (11).

The fundamental issue here is the construction of the reference data. An antenna radiation pattern may be used for the transmitter modeling which is mathematically achieved by locating a vertical Gaussian pattern, $g(x) = u(z_0, x)$, on a specified height. Then, the modal summation in (8) is used together with the orthonormality condition (10) and the number of modes and their excitation coefficients are derived numerically for a given error boundary. Note that, modal excitation coefficients are real if the antenna pattern has no vertical tilt (i.e., antenna pattern is horizontal, parallel to the flat-Earth). These modal excitation coefficients become complex when upslope or downslope tilt is introduced. Moreover, the modes are confined between the Earth's surface and modal caustics which depend on the mode number; the higher the mode, the higher the location of the caustic. Therefore, the number of modes used in the superposition directly depends on the antenna height.

Finally, vertical boundaries of the numerical integration during the modal excitation coefficient extraction from the orthonormality property increase as the mode number increases. The specification of the number of numerical integration steps for the calculation of modal

excitation coefficients is crucial. The code must adopt the number of integration steps automatically as the mode index increases.

Table 1 lists the number of modes required to establish a given Gaussian antenna pattern for a fixed error and antenna tilt. As seen from this table, the number of modes tremendously increases as the antenna tilt increases. It is quite inefficient to continue the modal summation procedure for the tilts beyond 10° .

Table 1: Number of modes used with respect to maximum initial field error $< 1e-8$ ($f = 300$ MHz, $h_s = 250$ m, $bw = 0.35$, $dM/dx = -600$ M/km)

Tilt angle ($^\circ$)	# of modes (N)	Tilt angle ($^\circ$)	# of modes (N)
0	19	6	2099
1	69	7	3114
2	191	8	4380
3	418	9	5984
4	795	10	7926
5	1342		

B. Single knife-edge problem and the four ray model

It appears that the surface duct model in Sec. III. A can be used within the paraxial region because the numerical instabilities and insufficiencies meet there during the generation of the reference data. The single-knife-edge problem, the four ray model (4Ray), and Fresnel integral representations [14] can be used as an alternative model from which reliable reference data can be generated. The scenario of this canonical problem is pictured in Fig. 5. Here, h_t , h_r , and h_w are the heights of the transmitter, receiver, and the knife-edge obstacle; d_1 and d_2 are the distances from source to obstacle and from obstacle to receiver, respectively.

Possible four rays are as follows: Ray 1 is the direct path between the transmitter and the receiver. Ray 2 is considered as the ray from the transmitter reflected from the right side of the knife-edge obstacle. This ray reaches the receiver directly or tip-diffraction may occur. Ray 3 is considered as the ray from the transmitter reflected from the left side of the knife-edge obstacle. Same as before, this ray also reaches the receiver

directly or tip-diffraction will occur. Ray 4 is considered as the ray from the transmitter reflected

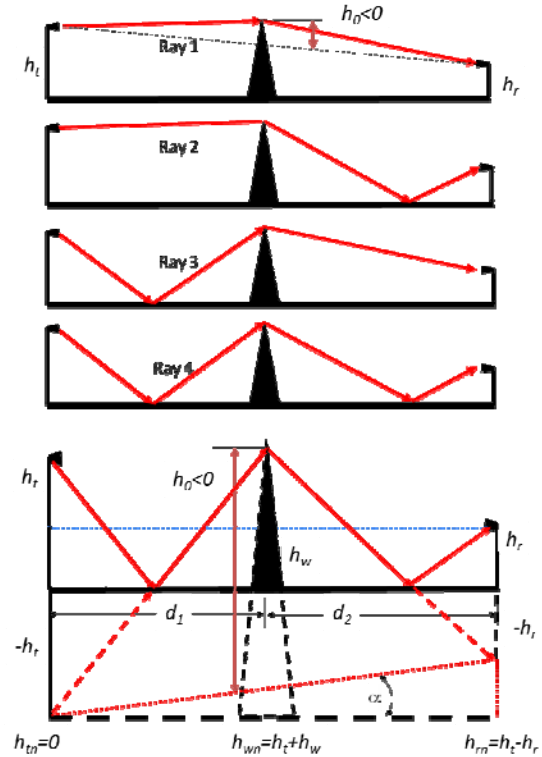


Fig. 5. (Top) The geometry of the flat-Earth and the single knife-edge problem. (Bottom) The construction of Ray 4 from the source/receiver images and h_0 .

from both the left side and the right side of the knife-edge obstacle.

The parameters of the Fresnel integrals are derived by using the image source/receiver for the reflected waves. The Fresnel clearance, the height of the knife-edge above the line-of-sight may be positive or negative [14]. When the direct ray between the transmitter and receiver intersects obstacle, h_0 is taken negative. The Fresnel integrals $C(v)$ and $S(v)$ are evaluated, where $v = h_0\sqrt{2}$ with h_0 equal to the ray clearance over the knife-edge. The pattern propagation factor (PF) is equal to:

$$F = \frac{E}{E_0} = \sum_{q=1}^4 E_q \exp(i\psi_q), \quad (12)$$

where $E_q = A(v_q)\Gamma_q$, $\Gamma_1 = 1$, $\Gamma_2 = \Gamma_R$, $\Gamma_3 = \Gamma_L$, $\Gamma_4 = \Gamma_L\Gamma_R$, and $\psi_q = \beta_q + (R_q - R_1)k_0$. Here,

$$A(v_q) = \sqrt{\frac{(C(v_q) + 0.5)^2 + (S(v_q) + 0.5)^2}{2}}, \quad (13)$$

for $C(v_q) = \int_0^v \cos(v_q^2) dv$, $S(v_q) = \int_0^v \sin(v_q^2) dv$; the distances of four rays are

$$R_q = \begin{cases} \sqrt{d^2 + (h_t - h_r)^2} & \text{for } q=1, q=3 \\ \sqrt{d^2 + (h_t + h_r)^2} & \text{for } q=2, q=4 \end{cases}, \quad (14)$$

$$\beta_q = \begin{cases} \arctan\left(\frac{S(v_q) + 0.5}{C(v_q) + 0.5}\right) - \frac{\pi}{4} & \text{if } C(v_q) \geq -0.5 \\ \arctan\left(\frac{S(v_q) + 0.5}{C(v_q) + 0.5}\right) + \frac{3\pi}{4} & \text{if } C(v_q) < -0.5 \end{cases}, \quad (15)$$

and the complex reflection coefficients, for the horizontal and vertical polarizations, respectively, are:

$$\Gamma = \frac{\sin(\theta) - \sqrt{\varepsilon - \cos^2(\theta)}}{\sin(\theta) + \sqrt{\varepsilon - \cos^2(\theta)}}, \quad \Gamma = \frac{\varepsilon \sin(\theta) - \sqrt{\varepsilon - \cos^2(\theta)}}{\varepsilon \sin(\theta) + \sqrt{\varepsilon - \cos^2(\theta)}}, \quad (16)$$

where $\varepsilon = \varepsilon_r - i60\sigma_g \lambda$, σ_g is the conductivity and ε_r is the relative permittivity of ground, θ is the angle of incidence in radians. The ray clearances for the four rays are:

$$h_{01} = \sqrt{\frac{2d}{\lambda d_1 d_2}} \left(-h_t + \frac{(h_r - h_t)d_1}{d} - h_w \right), \quad (17a)$$

$$h_{02} = \sqrt{\frac{2d}{\lambda d_1 d_2}} \left(-h_t + \frac{(h_r + h_t)d_1}{d} - h_w \right), \quad (17b)$$

$$h_{03} = \sqrt{\frac{2d}{\lambda d_1 d_2}} \left(h_t + \frac{(-h_r - h_t)d_1}{d} - h_w \right), \quad (17c)$$

$$h_{04} = \sqrt{\frac{2d}{\lambda d_1 d_2}} \left(-h_t + \frac{(h_t - h_r)d_1}{d} - h_w \right). \quad (17d)$$

IV. VALIDATION, VERIFICATION AND CALIBRATION (VV&C)

VV&C starts with the model validation. The SSPE and FEMPE codes are based on one-way, forward propagation PE model which neglects back-scattered waves. This is not a serious limitation as long as one is interested in path losses between a transmitter and a receiver. Another limitation of the PE model is that, both narrow and wide angle PE models are valid within paraxial region. This should be taken into account for waves propagating upwards/downwards with some tilts and/or for propagation paths having longitudinally irregular terrain profiles with certain terrain slopes. Proper discretization (i.e., range and height step sizes, Δz and Δx , respectively) is essential in numerical simulations.

These are important issues that should be tested during the VV&C procedure.

The first VV&C example is presented in Fig. 6. Here, 3D visualization of both analytical and numerical solutions is presented where the transmitter contains two Gaussian patterns (i.e., two antennas) at 200m and 400m, with -0.5° and 0.5° tilts, respectively. In Fig. 6b, vertical field profiles at two different ranges obtained with all three (analytical, SSPE, and FEMPE) codes, are shown. Excellent agreement illustrates the success and completeness of the VV&C procedure.

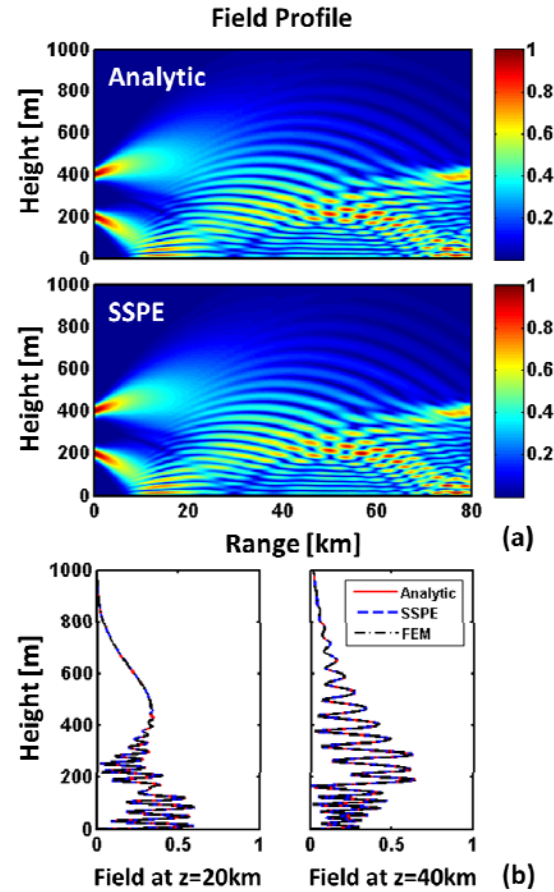


Fig. 6. (a) SSPE and analytic propagators with tilted waves at 200m and 400m with -0.5° , 0.5° tilts, respectively, (b) vertical field profiles at two different ranges ($dM/dx = -600$ M/km).

Obviously, the PE codes can be tested and calibrated against the numerically generated reference data obtained from analytical exact model for tilts up to 10° at most. Beyond that, SSPE and FEMPE can only be tested against some

other methods or using some physical electromagnetic reality. One way of testing narrow angle (6) and wide angle (7) PE representations is to tilt up or down the antenna pattern up to 40° - 45° . The modal summation procedure for this example shows that, although an exact mathematical solution is at hand, it might be extremely difficult to produce numerical reference data for the VV&C tests. An example for this case is given in Fig. 7. Since the SSPE result is exactly the same with the FEMPE result, it is not included here.

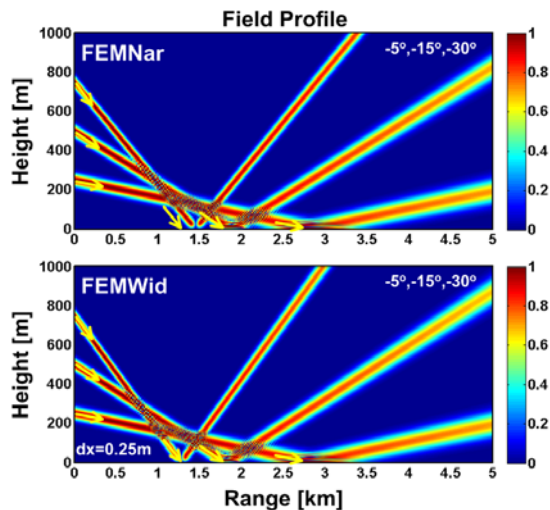


Fig. 7. Narrow and wide angle FEMPE propagators for -5° , -15° , -30° tilted waves at 250m, 500m, 700m, respectively.

Here, a three antenna transmit system is used. The antennas are located at 250m, 500m, and 750m heights with -5° , -15° , -30° tilts, respectively. The frequency is 300MHz. The tilt down waves hit the ground at 2.85km, 1.86km, 1.29km for -5° , -15° , -30° , respectively (the effects of refractivity variations at these ranges are almost negligible and waves propagate almost as in free space with straight lines). Note that vertical step should satisfy $\Delta x \leq \lambda / (2 \sin(2\alpha_{\max}))$ where α_{\max} is the maximum tilt (or terrain slope if irregular terrain is present). At 300MHz (i.e., $\lambda = 1$ m) $\Delta x \leq 1$ m for -15° tilt, but $\Delta x \leq 0.5$ m for -45° tilt. The 3D plots in this figure are produced with $\Delta x = 0.25$ m for SSPE and FEMPE; therefore, the discretization satisfies the tilt requirements. It is clearly observed from these plots that both narrow and wide angle PE models can handle tilts up to $\pm 15^\circ$, but only wide angle PE can handle tilts

beyond these values. Note that the computation times for this example for the selected list of parameters with the narrow and wide angle SSPE are 48s and 51s, and with the narrow and wide angle FEMPE are 2844s and 3350s, respectively.

The VV&C of the PE tools out of the paraxial region is conducted on the single knife-edge model given in Sec. III. B. The last three figures belong to this VV&C procedure. In Fig. 8, 3D field maps generated via the SSPE tool and the 4Ray model. The scenario belongs to one-way propagation for horizontal polarization over PEC ground with 75m height-wall at 15km range. The line source is at 15m height at $z=0$. The FEMPE result is exactly the same with the SSPE map, therefore it is not included in this figure.

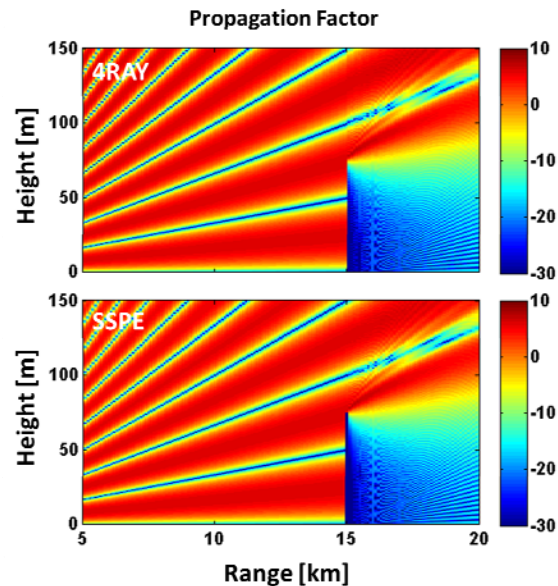


Fig. 8. One-way propagation for horizontal polarization over PEC ground with 75m height-wall at 15km range. The propagation factor vs. range/height for a given source (at 20m height, 0km range): $f=3$ GHz, $\Delta x=0.1$ m, $\Delta z=50$ m.

The PFs vs. height in front of and beyond the wedge-type obstacle are plotted in Fig. 9. Here, four vertical field profiles obtained with both SSPE and four ray model are plotted. The first plot on the left belongs to the interference region (before the obstacle); the other three are in the diffraction region (beyond the obstacle). As observed, excellent agreement is obtained in all of the plots. Note that the height of the edge of the obstacle is 75m and the distances of these three profiles from the obstacle are 100m, 1km, and

3km, respectively. The maximum diffraction angles of these three are around 36.9° , 4.3° , and 1.5° , respectively. It is expected that the PE models are not effective and accurate for the angles beyond 30° - 35° . As observed, the PE models are insufficient in modeling the diffracted fields in the deep shadow regions.

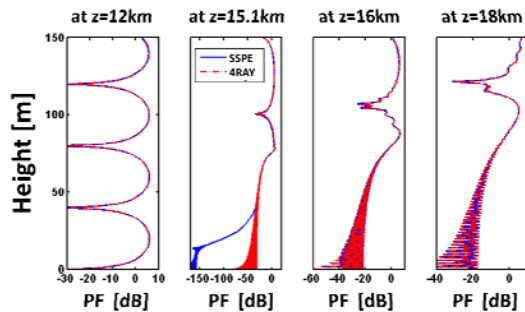


Fig. 9. The PF vs. height at four ranges; 12km, 15.1km, 16km, and 18km ($f=3\text{GHz}$, solid: 4Ray, dashed: SSPE, $\Delta x=0.1\text{m}$, $\Delta z=50\text{m}$).

V. CONCLUSIONS

Model validation, data verification, and code calibration (VV&C) is an important engineering task. Engineers deal with real-life problems; they design, test, measure, simulate, etc. The first step is the definition of the problem; the solution cannot be found without clear definition of the problem. In electromagnetics, Maxwell's equations plus BCs well-define the problem at hand. Mathematically speaking, the existence and uniqueness of the solution is already there once Maxwell's equations are stated with the right BCs. Therefore, the conceptual (mathematical) model is already at hand in electromagnetics. The challenge is the numerical computation. Unfortunately, only a few problems with idealized conditions have mathematical exact solutions; therefore one needs to introduce approximations, assumptions, simplifications, etc., which yield a variety of different conceptual models. The VV&C procedure starts with the choice of the right model and necessitates the validation procedure. Then, the computer coding and verification procedure come. The final stage is the calibration.

The VV&C procedure is discussed systematically over a 2D groundwave propagation problem. The flat-Earth above PEC surface with vertically decreasing refractivity profile (without and with a single knife-edge obstacle) is taken into

account for this purpose. The well-known PWE model is chosen as the conceptual model. Both split-step and finite-element based PWE codes are developed. Numerical data generated via these models are compared against analytical exact results. Difficulties in producing numerical data for the analytical exact solutions and in calibration are presented.

Note that the VV&C procedure discussed in Sec. IV automatically answers the crucial questions asked at the beginning of Sec. III. The terrain profiles used in Figs. 3 and 4 are synthetically generated; measurements along these paths are not possible. Furthermore, a mathematical/ analytical model is not available because of the complexity of the boundary conditions there. Therefore, reference data (which can only be obtained either from a reliable analytical model or measurements) cannot be generated. All that can be done is to do comparisons among different numerical models/packages. For these kinds of problems (where no reference data could be generated) results should be presented with caution. The results of different numerical models/packages might show a perfect agreement but still be totally erroneous [11-13].

REFERENCES

- [1] G. Apaydin and L. Sevgi, "Validation, verification, and calibration in applied computational electromagnetics," *26th International Review of Progress in Applied Computational Electromagnetics*, Tampere, Finland, pp. 679-684, Apr. 2010.
- [2] L. Sevgi, *Complex Electromagnetic Problems and Numerical Simulation Approaches*, IEEE Press/Wiley, Piscataway, NJ, Jun. 2003.
- [3] M. A. Leontovich and V. A. Fock, "Solution of propagation of electromagnetic waves along the Earth's surface by the method of parabolic equation," *Journal of Physics of the USSR*, vol. 10, pp. 13-23, 1946.
- [4] M. F. Levy, *Parabolic Equation Methods for Electromagnetic Wave Propagation*, The Institution of Electrical Engineers, London, U.K., 2000.
- [5] D. J. Thomson and N. R. Chapman, "A wide-angle split-step algorithm for the parabolic equation," *J. Acoust. Soc. Am.*, vol. 74, no. 6, Dec. 1983.

- [6] L. Sevgi, "Modeling and simulation strategies for electromagnetic wave propagation in complex environments: Groundwave path loss prediction virtual tools," *IEEE Trans. Antennas Propagat.*, vol. 55, no. 6, pp. 1591-1598, Jun. 2007.
- [7] L. Sevgi, C. Uluisik, and F. Akleman, "A Matlab-based two-dimensional parabolic equation radiowave propagation package," *IEEE Antennas and Propag. Mag.*, vol. 47, no. 4, pp. 164-175, Aug. 2005.
- [8] D. Huang, "Finite element solution to the parabolic wave equation," *J. Acoust. Soc. Am.* vol. 84, no. 4, pp. 1405-1413, Oct. 1988.
- [9] K. Arshad, F. A. Katsriku and A. Lasebae, "An investigation of tropospheric radio wave propagation using finite elements," *WSEAS Trans. Commun.*, vol. 4, no. 11, pp. 1186-1192, Nov. 2005.
- [10] G. Apaydin and L. Sevgi, "The split step Fourier and finite element based parabolic equation propagation prediction tools: canonical tests, systematic comparisons, and calibration," *IEEE Antennas and Propag. Mag.*, vol. 52, no. 3, Jun. 2010.
- [11] G. Apaydin and L. Sevgi, "A novel split-step parabolic equation package for surface wave propagation prediction along multi-mixed irregular terrain paths," *IEEE Antennas and Propag. Mag.*, vol. 52, no. 3, Aug. 2010.
- [12] G. Apaydin and L. Sevgi, "FEM-based surface wave multi-mixed-path propagator and path loss predictions," *IEEE Antennas Wireless Propag. Lett.*, vol. 8, pp. 1010-1013, 2009.
- [13] G. Apaydin and L. Sevgi, "Numerical investigations of and path loss predictions for surface wave propagation over sea paths including hilly island transitions," *IEEE Trans. Antennas Propagat.*, vol. 58, pp. 1302-1314, Apr. 2010.
- [14] M. L. Meeks, *Radar Propagation at Low Altitudes*, Artech House, 1982.



Gokhan Apaydin received the B.S., M.S., and Ph.D. degrees in Electrical and Electronics Engineering from Bogazici University, Istanbul, Turkey, in 2001, 2003, and 2007, respectively.

He was employed as a Teaching and Research Assistant by Bogazici University from 2001 to 2005, and a Project and Research Engineer by Applied Research and Development, University of Technology, Zurich, Switzerland, from 2005 to 2010. Since 2010, he has been with Zirve University, Turkey. He has been working several research projects on electromagnetic scattering, the development of finite element method for electromagnetic computation, propagation, positioning, digital signal processing, filter design, and related areas. He has (co)authored 14 journals, 26 conference papers, and many technical reports at the University of Applied Science Zurich.



Levent Sevgi received the Ph.D. degree from Istanbul Technical University and Polytechnic Institute of New York, in 1990. Prof. Leo Felsen was his advisor.

He was with Istanbul Technical University (1991–1998), TUBITAK-MRC, Information Technologies Research Institute (1999–2000), Weber Research Institute/Polytechnic University in New York (1988–1990), Scientific Research Group of Raytheon Systems, Canada (1998 – 1999), Center for Defense Studies, ITUV-SAM (1993 –1998, 2000–2002). Since 2001, he has been with Dogus University. He has been involved with complex electromagnetic problems and systems for more than 20 years. His research study has focused on propagation in complex environments, analytical and numerical methods in electromagnetic, EMC/EMI modeling and measurement, radar and integrated surveillance systems, surface wave HF radars, FDTD, TLM, FEM, SSPE, and MoM techniques and their applications, RCS modeling, bio-electromagnetics. He is also interested in novel approaches in engineering education, teaching electromagnetics via virtual tools. He also teaches popular science lectures such as science, technology, and society.

Prof. Sevgi is a Fellow of the IEEE, the writer/editor of the "Testing ourselves" Column in the IEEE Antennas and Propagation Magazine, a member of the IEEE Antennas and Propagation Society Education Committee, and the "Scientific Literacy" column writer of the IEEE Region 8 Newsletter.